JOURNAL OF MATERIALS SCIENCE 13 (1978) 571–579

# Mechanical properties of unidirectionally transformed Cu-In alloys

B. G. MELLOR*, D. V. EDMONDS
*Department of Metallurgy and Materials Science, University of Cambridge, Cambridge, UK*

Comprehensive hardness measurements and limited tensile tests have been made on eutectoid and off-eutectoid Cu–In alloys. The alloys were transformed by unidirectional heat-treatment techniques using a range of imposed growth rates which resulted in alignment of the pearlite microstructure and a range of interlamellar spacing. Room temperature hardness of the as-transformed alloys was found to vary linearly as a function of $\lambda^{-1/2}$, where $\lambda$ is the pearlite interlamellar spacing; the alloys were calculated to have cooled from the decomposition temperature at rates in the range 0.047 to 18.6 K min$^{-1}$, which could result in variations of precipitation/coarsening reactions in the pearlitic phases contributing towards strength, as well as the lamellae interfaces. Hardness was also measured as a function of temperature and indicated a change in strengthening mechanism at ~550 K, thought to indicate the temperature above which no significant strengthening was contributed by the pearlitic interfaces. Tensile failure of the lamellar structure occurred in a manner identical to directionally aligned Al–$CuAl_2$ eutectics.

## 1. Introduction

During the last decade considerable interest has been shown in the possible use of unidirectionally solidified eutectic alloys for certain engineering applications [1–3]. Consequently, the mechanical properties of eutectic microstructures in a wide range of alloys have been investigated [4, 5]. More recently, it has also proved possible to produce aligned eutectoid microstructures by the use of unidirectional heat-treatment techniques, thus broadening the range of alloys which could be considered for their unidirectional mechanical or physical properties. The eutectoid alloys studied so far include Cu–Al [6–8], Cu–In [7, 9], Ni–In [7, 10], Zn–Al [11], Fe–Al [12], Co–Si [7, 10, 13] and Fe–C [14–18].

Apart from the Fe–C system, quite limited studies have so far been made of the mechanical properties of eutectoid microstructures, and even less of aligned microstructures. Thus, the present paper reports comparative studies of hardness as a function of microstructure in Cu–In alloys which have been transformed by unidirectional heat-treatment techniques. The most popular method used to study mechanical property variations as a function of microstructure is traditionally that of tensile testing. However, the production by unidirectional heat-treatment techniques of sufficient material for tensile specimens of the necessary quality, possibly in "bicrystal" form, and for which the microstructure has been carefully analysed, would require considerable experimental time. Consequently, for strength comparisons hardness testing techniques were employed on small specimens which had been fully characterized previously by optical and electron microscopy [9]. Limited tensile tests were carried out only to observe the two-phase deformation and fracture behaviour as a function of temperature.

## 2. Experimental procedures

### 2.1. Hardness measurements

Macrohardness measurements were made on transverse sections of eutectoid Cu–31.36 wt % In, previously used to examine transformation

*Now at Departamento de Metalurgia, Universidad Complutense de Madrid, Spain.

velocity/interlamellar spacing relationships [9], with a standard Vickers hardness machine using a load of 10 kg. A minimum of five indents were made on each specimen. Microhardness measurements were also obtained with a Lietz microhardness indenter, using a load of 0.3 kg. One diagonal of the microhardness indent was always aligned parallel to the pearlite lamellae.

Hypoeutectoid Cu–30 wt % In and hypereutectoid Cu–32.3 wt % In were transformed unidirectionally at 1.6 mm h$^{-1}$. A description of the unidirectional heat-treatment technique has been given previously [9]. Transverse sections of the aligned structures were metallographically prepared and high-temperature microhardness tests carried out in an apparatus designed by Gove [19], which allowed the simultaneous heating of specimen and indenter in an argon atmosphere. For pearlite and proeutectoid $\alpha$-phase, a load of 0.1 kg was used, while for the smaller proeutectoid $\delta$-phase a load of 0.025 kg was necessary. Indentation times of 15 ± 0.1 sec were employed.

## 2.2. Tensile tests

Hounsfield No. 11 tensile specimens were ground from specimens of unidirectionally transformed Cu–30 wt % In alloy. Tensile testing was carried out in air with an Instron testing machine using a cross-head speed of 0.1 mm min$^{-1}$.

# 3. Results

Fig. 1 illustrates the pearlitic structure obtainable in the Cu–In alloys, and the general alignment of the phases by the unidirectional heat-treatment technique. The results of Vickers microhardness measurements as a function of transformation velocity for the Cu–31.36 wt % In alloy are presented in Table I; also tabulated are the interlamellar spacing measurements previously made on the specimens by both optical and electron microscopy techniques [9].

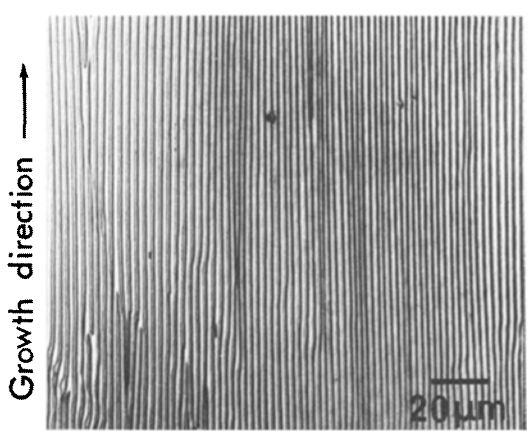


*Figure 1* Longitudinal section of Cu–31.36 In unidirectionally transformed at 0.4 mm h$^{-1}$.

TABLE 1 Vickers hardness of Cu–31.36 In as a function of transformation velocity and interlamellar spacing.

| Transformation velocity (mm h$^{-1}$) | Minimum interlamellar spacing, $\lambda_{MIN}$ ($\mu$m) | Average interlamellar spacing, $\lambda_{AV}$ ($\mu$m) | Vickers hardness (V.P.N.) |
|---|---|---|---|
| 0.2 | 2.82 | 3.25 | 328 ± 6 |
| 0.27 | 1.68 | 2.00 | 319 ± 16 |
| 0.4 | 1.03 | 1.46 | 317 ± 13 |
| 1.2 | 0.790 | 1.17 | 333 ± 11 |
| 1.6 | 0.650 | 0.790 | 343 ± 12 |
| 3.2 | 0.364 | 0.470 | 363 ± 9 |
| 5.0 | 0.340 | 0.440 | 355 ± 9 |
| 20.0 | 0.246 | 0.350 | 380 ± 14 |
| 60.0 | 0.170 | 0.220 | 415 ± 16 |
| 80.0 | 0.117 | 0.138 | 409 ± 12 |

TABLE II Vickers microhardness measurements on Cu–31.36 In.

| Transformation velocity (mm h$^{-1}$) | Vickers microhardness (V.P.N.) | | Average vickers micro-harndess (V.P.N.) | Vickers macro-hardness (V.P.N.) |
|---|---|---|---|---|
| | Parallel to lamellae | Normal to lamellae | | |
| 0.27 | 356 ± 5 | 302 ± 7 | 329 ± 6 | 319 ± 16 |
| 1.6 | 377 ± 22 | 295 ± 9 | 336 ± 15 | 343 ± 12 |

The results of Vickers microhardness measurements as a function of two transformation velocities are given in Table II. An example of the microhardness indents obtained is shown in Fig. 2a, and it can be seen that the two diagonal lengths are not the same, depending on whether the diagonal is parallel or normal to the pearlite lamellae. This difference in diagonal lengths is reflected in the measurements given in Table II, which show that the hardness in a direction parallel to the lamellae averages approximately 23% higher than in a direction normal to the lamellae. However, the hardness calculated from the average diagonal lengths is also given in Table II and is seen to be approximately equal to the value found for the randomly oriented macrohardness measurements.

Fig. 2b illustrates a hardness indent after further polishing of the surface. The lamellae are

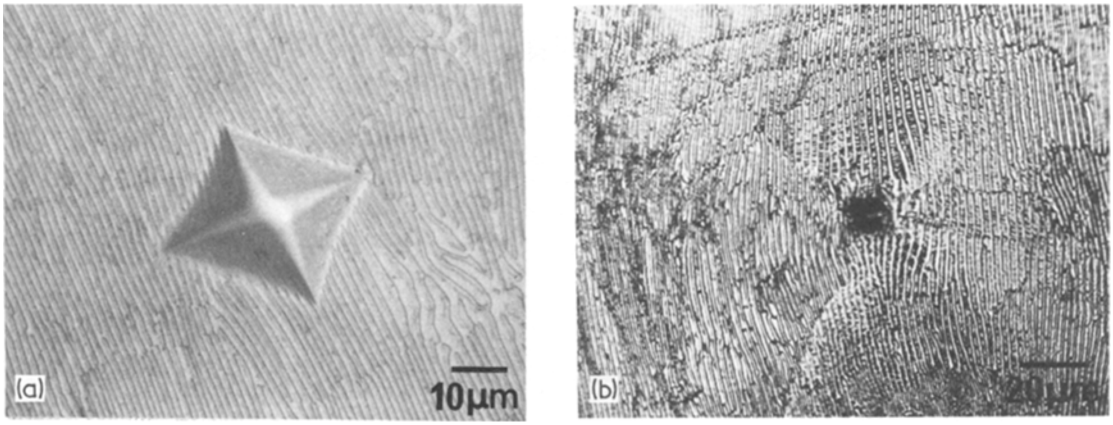


*Figure 2* Microhardness indents on transverse sections of Cu–31.36 In (a) unidirectionally transformed at 0.27 mm $h^{-1}$, and (b) unidirectionally transformed at 0.4 mm $h^{-1}$ and polished after indenting.

TABLE III Vickers microhardness as a function of temperature for α-phase, δ-phase and pearlite unidirectionally heat treated at 1.6 mm $h^{-1}$.

| Temperature | Vickers | Hardness | (V.P.N.) |
|---|---|---|---|
| (K) | α | δ | Pearlite |
| 298 | 102 ± 4 | 430 ± 50 | 332 ± 14 |
| 373 | 100 ± 4 | 410 ± 40 | 324 ± 15 |
| 473 | 97 ± 8 | 398 ± 20 | 296 ± 26 |
| 573 | 84 ± 4 | 354 ± 12 | 226 ± 8 |
| 673 | 73 ± 5 | 156 ± 5 | 97 ± 8 |
| 773 | 36 ± 4 | | 42 ± 3 |

observed to have bent around the indenter, and some cracking of the δ-phase can also be detected.

The microhardness of the constituent phases in the hypo- and hyper-eutectoid Cu–In alloys as a function of temperature are given in Table III. The hardness for the δ-phase was obtained using a load of 0.025 kg, but to enable comparison has been corrected to the value expected for a load of 0.10 kg as was used for the α-phase and the pearlite. At 773 K the hardness of the δ-phase could not be determined as the indent size was approximately the same width as that of the δ-phase. Fig. 3 illustrates typical indents in the proeutectoid α- and δ-phase, and in the pearlite. It can also be seen from Fig. 3a that continuous precipitation has occurred in the proeutectoid α-phase. In some cases this precipitation also appeared to have occurred by a discontinuous reaction.

Typical tensile stress–strain curves exhibited by the unidirectionally heat-treated Cu–30 wt % In containing approximately 10% proeutectoid α-phase, are shown in Fig. 4. At 293 K failure occurred in an apparently brittle manner before

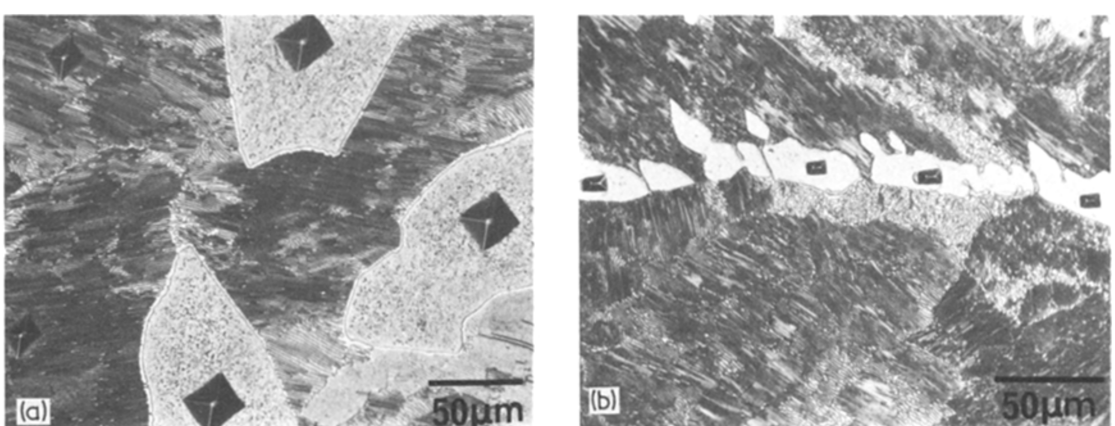


*Figure 3* Room-temperature microhardness indents in (a) proeutectoid α-phase in Cu–30 In, and (b) proeutectoid δ-phase in Cu–32.3 In.

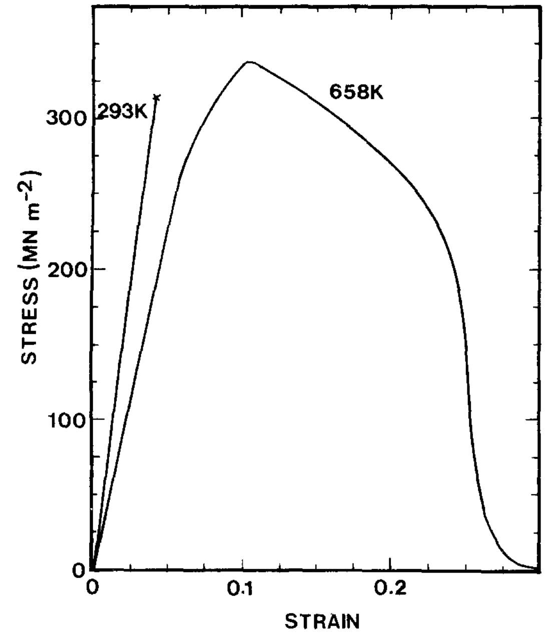


*Figure 4* Nominal stress–strain curves at 293 K and 658 K for unidirectionally transformed Cu–30 In.

any deviation from linearity in the stress–strain curve was detected, while at 658 K extensive plastic deformation occurred. The appearance of specimens fractured at 293 and 658 K, respectively, is shown in Fig. 5, and illustrates the change from brittle to ductile failure. The macroscopic fracture surface can also be observed to change from transverse at 293 K to approximately 45° at 658 K.

The microscopic appearance of the fracture surface obtained at 293 K shows parallel ridges (Fig. 6a). A longitudinal section of the fractured specimen is shown in Fig. 6b and illustrates cracking of the $\delta$-phase ahead of a secondary crack beneath the main fracture. Mid-plane cleavage of the $\delta$-phase was also occasionally observed. This secondary cracking occurred only beneath the main fracture and not elsewhere in the gauge length. It can be seen that the width of the parallel ridges on the fracture surface is comparable to the interlamellar spacing. The failure mechanism at 293 K thus appears to be caused predominantly by transverse brittle cleavage of the $\delta$-phase, followed by failure of the copper-rich $\alpha$-phase which is drawn out by ductile shear to result in the ridged profile of the fracture surface.

At 658 K the fracture surface appeared more ductile, but still showed some parallel ridges, which although of a separation not comparable to the interlamellar spacing may still be related to the lamellar microstructure (Fig. 7a). Longitudinal sections showed deformation of the lamellae (Fig. 7b), and also revealed voids nucleated at the interfaces of the proeutectoid $\alpha$-phase as well as apparently in the pearlite matrix.

## 4. Discussion

Table I shows that hardness increases as transformation velocity increases and interlamellar spacing decreases. The practice has arisen in recent years of attempting to relate mechanical property data

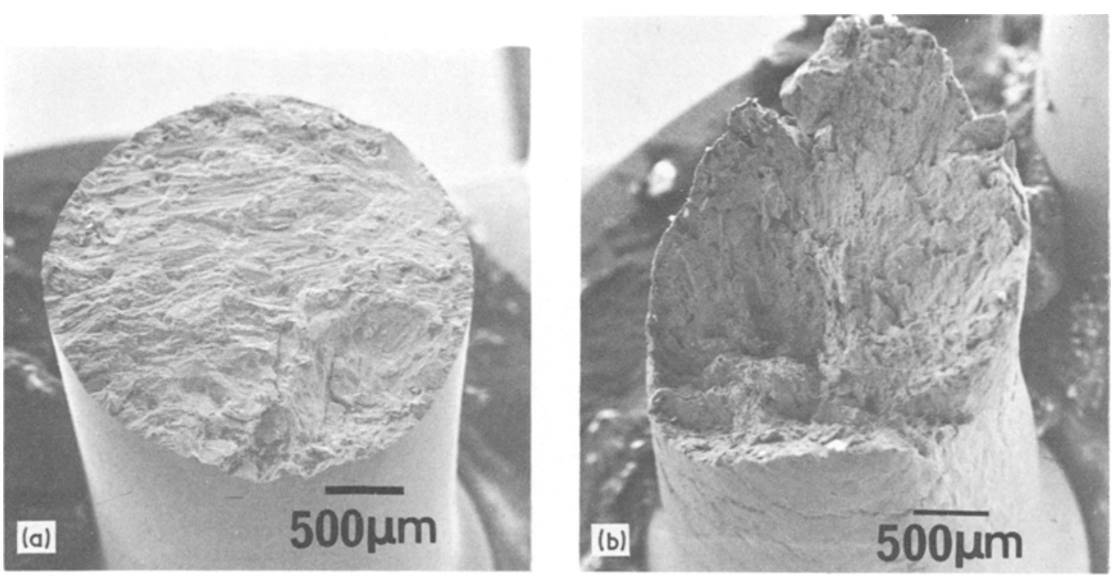


*Figure 5* Macroscopic appearance of fracture of unidirectionally transformed Cu–30 In tested at (a) 293 K, and (b) 658 K.

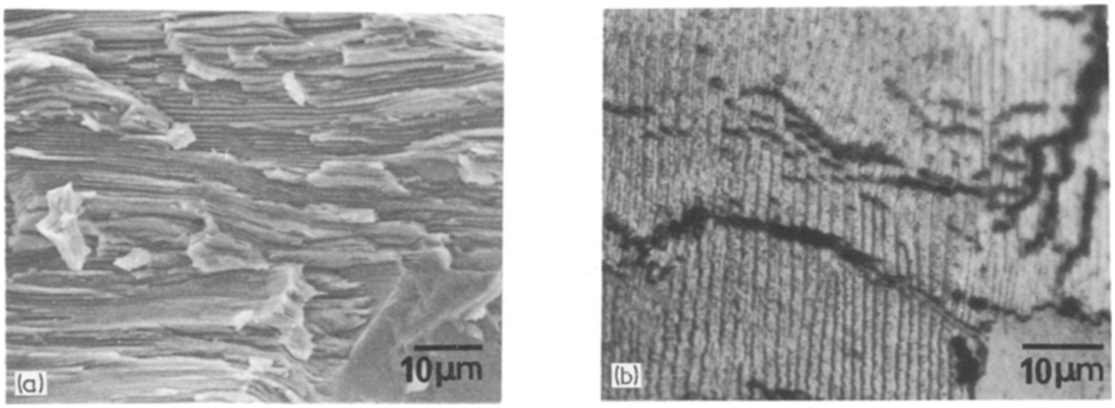


*Figure 6* Unidirectionally transformed Cu–30 In tested at 293 K showing (a) fracture surface, and (b) longitudinal section close to the fracture face.

obtained from eutectic alloys to a measurable microstructural feature, the most obvious being the interlamellar spacing. Often a Hall–Petch relationship has been shown, but this method of interpretation has been criticised on the grounds that a significant contribution to strengthening may not be directly related to the interlamellar spacing [5, 20]. Furthermore, the dislocation mechanism implicit in deriving the Hall–Petch equation, that is, the transmission of stress through structural boundaries by dislocation pile-ups at the boundaries, is not necessarily applicable to the case of a lamellar eutectic/eutectoid microstructure. Other yielding mechanisms, for example, dislocation generation at lamellar faults, are more likely and need not be related to the interlamellar spacing [5, 20].

However, for comparative purposes in a single system, there is some advantage in finding a simple mathematical relationship between a measured mechanical property and a microstructural feature which is altered by variation in heat-treatment temperature, or in the present case by transformation velocity, and which is known to change significantly the measured property. Consequently, the hardness data in Table I were plotted as a function of $\lambda^{-1}$, $\lambda^{-1/2}$, $\lambda^{-1/3}$ and $\lambda$ (Fig. 8), all of which have been used in other investigations [21–29]. Linear regression analysis of all the data points for both the minimum and average interlamellar spacing versus hardness results identified the best fit from a V.P.N. versus $\lambda^{-1/2}$ relationship. Fig. 8 also shows that all the relationships tested, with the possible exception of V.P.N. versus $\lambda$, yielded straight lines in the region of higher $\lambda$ values. A $\lambda^{-1/2}$ relationship has frequently been obtained for both yield strengths and hardness data in lamellar microstructures. It is thus likely that simple hardness measurements can be used to reflect accurately the changes to be

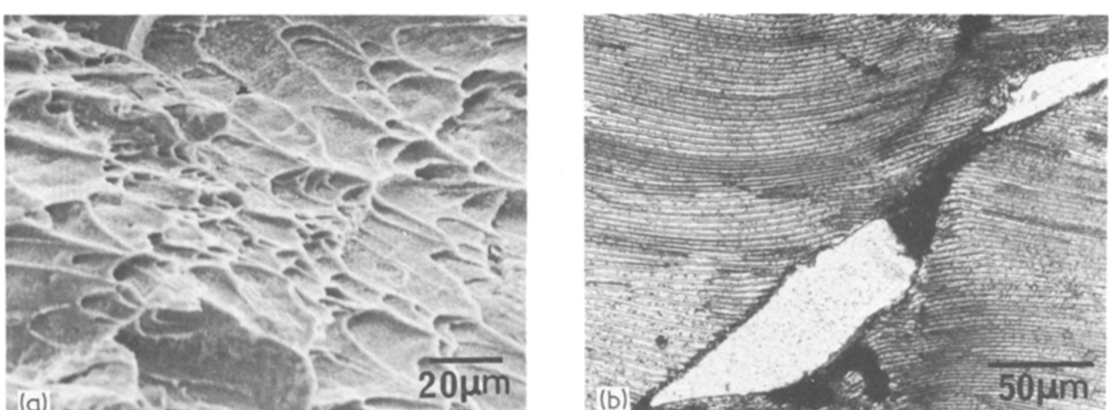


*Figure 7* Unidirectionally transformed Cu–30 In tested at 658 K showing (a) fracture surface, and (b) longitudinal section close to the fracture face.

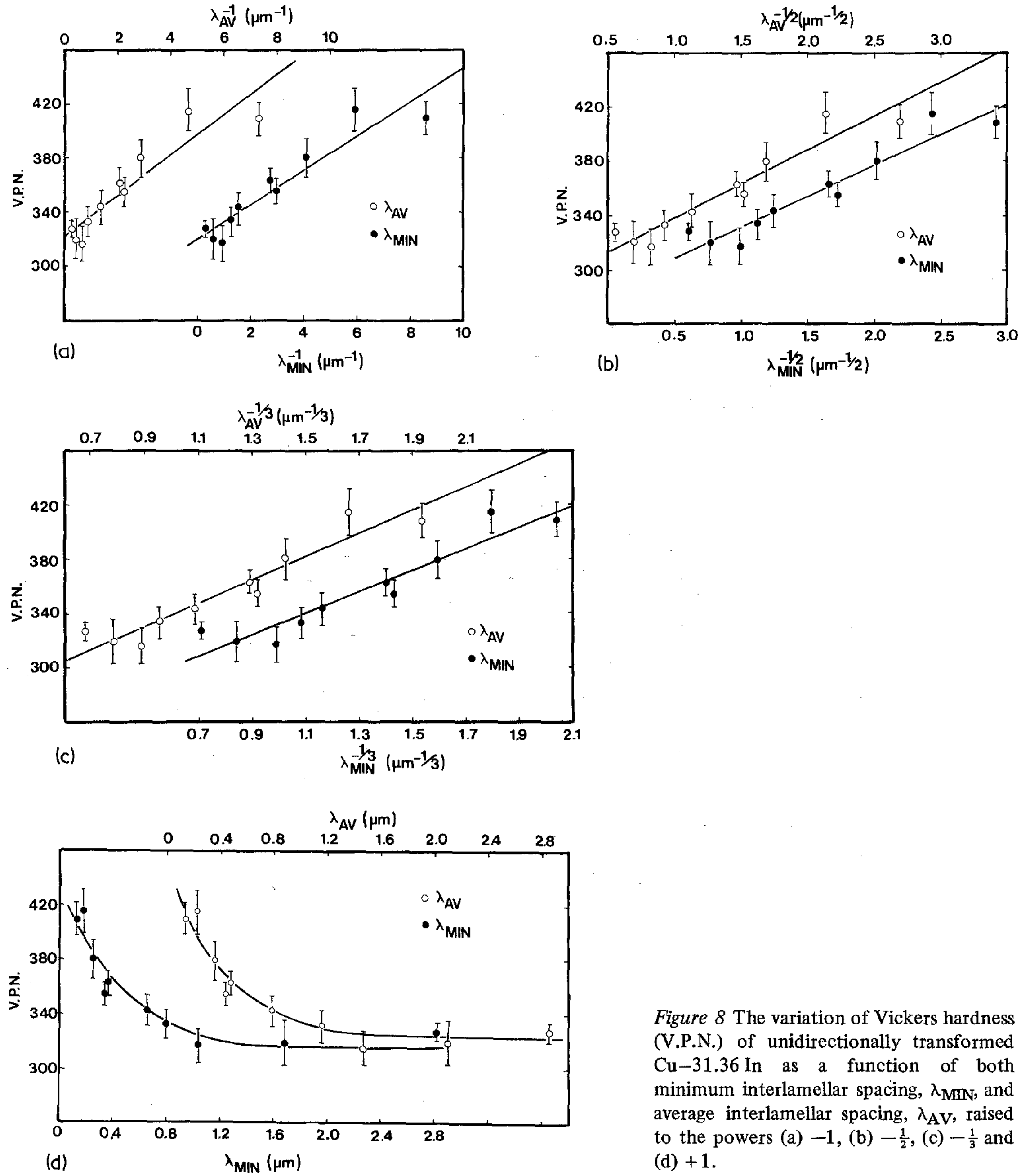


*Figure 8* The variation of Vickers hardness (V.P.N.) of unidirectionally transformed Cu–31.36 In as a function of both minimum interlamellar spacing, $\lambda_{MIN}$, and average interlamellar spacing, $\lambda_{AV}$, raised to the powers (a) $-1$, (b) $-\frac{1}{2}$, (c) $-\frac{1}{3}$ and (d) $+1$.

expected in other mechanical properties, e.g. yield stress, as a function of microstructure, a view which is becoming more widely accepted [5, 30].

It has recently been argued [5, 20] that much of the mechanical property measurements made on unidirectionally solidified eutectics reflect not only the variation in interlamellar spacing, but also other changes caused by variations in thermal history of the phases brought about by specimen cooling rates from the solidification temperature, which alter as a function of the growth velocity. These include thermal stresses, dislocation densities, solute supersaturations and precipitation.

The specimen cooling rate, $R$, in a unidirectional heat-treatment experiment can be estimated from the relationship

$$R = GV \qquad (1)$$

where $G$ is the temperature gradient and $V$ the specimen velocity (this assumes that the specimen velocity is equivalent to the growth velocity). Thus in the present work where Cu–In eutectoid was unidirectionally transformed at velocities in the range 0.2 to $80\,\mathrm{mm\,h^{-1}}$ under a temperature gradient of approximately $14\,\mathrm{K\,mm^{-1}}$, the specimen cooling rates are estimated from Equation 1 to be in the range 0.047 to $18.6\,\mathrm{K\,min^{-1}}$. From this analysis we may conclude that the cooling rates experienced by Cu–In eutectoid specimens during unidirectional heat-treatment range from very slow cooling to intermediate cooling rates and are very much slower than the customary quench rates of conventional heat treatment (e.g. $600\,\mathrm{K\,min^{-1}}$ described as a slow quench by Davies and Hellawell [22]). Consequently, it is more likely that this range of cooling rates will influence precipitation and/or coarsening reactions rather than lead to quenched-in non-equilibrium conditions such as high solute supersaturations. Thus the question becomes not one of whether the cooling rate is sufficiently slow to relieve solute supersaturation, but how it influences the precipitation and/or coarsening reactions which occur. It is therefore interesting that some evidence of precipitation during continuous cooling from the unidirectional transformation temperature was observed in the present study, although this occurred in the pro-eutectoid $\alpha$-phase as shown in Fig. 3a. Both continuous and discontinuous precipitation in Cu supersaturated with In have been considered previously by several investigators [31–34], and it has been shown [33] that continuous precipitation on a fine scale (not resolvable optically) can give rise to marked increases in hardness of the $\alpha$-phase, the value of hardness depending on both the ageing temperature and time. Consequently, although the empirical relationship found between hardness and interlamellar spacing for the Cu–In eutectoid in the as-transformed state corresponds to the Hall–Petch relationship, the true dependence of hardness on interlamellar spacing could well be masked by age-hardening or coarsening effects, implying that the Hall–Petch strengthening mechanism need not necessarily be operative in this system.

The microhardness results showed that the hardness in a direction parallel to the pearlite lamellae was greater than in a direction normal to the lamellae. This anisotropy is consistent with a previous study of the $Al–CuAl_2$ lamellar eutectic [25], where the yield stress parallel to the lamellae was found to be higher than normal to the lamellae. In the present work it is shown that the lamellae bend to accommodate the deformation of the indenter in the normal direction. In the parallel direction, however, it is likely that more of the load is transferred by interface shear stresses to the stronger $\delta$-phase, which is protected from plastic failure or fracture by the constraint of the softer $\alpha$-phase and a strong interfacial bond. This behaviour indicates the possible benefits to be obtained from the mechanical strength of aligned eutectoid microstructures, which may therefore prove worthy of further study.

It has been shown that the temperature dependence of hardness($H$) is well represented by an empirical function of the form

$$H = Ae^{-BT} \qquad (2)$$

where $A$ and $B$ are constants and $T$ is the testing temperature [35]. Fig. 9a shows the results of

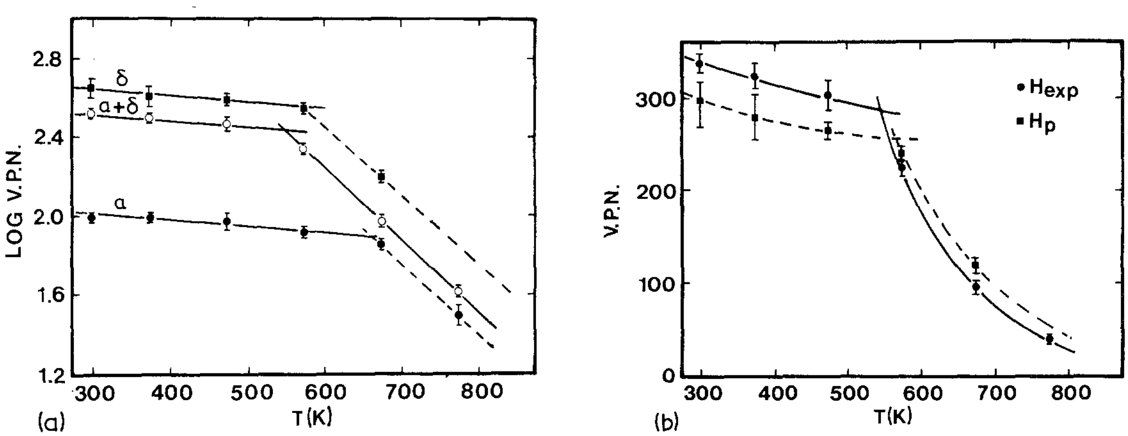


*Figure 9* Microhardness as a function of temperature; (a) hardness of $\alpha$-phase, $\delta$-phase and pearlite, and (b) experimental ($H_{exp}$) and calculated ($H_p$) hardnesses of pearlite.

plotting log V.P.N. versus $T$. For the $\alpha + \delta$ pearlite the experimental points are observed to fall on two straight lines which intersect at 553 K. For the $\alpha$- and $\delta$-phases the experimental points lie on straight lines at low temperatures, whilst the two points corresponding to the measured hardnesses at the highest testing temperature deviate from the straight lines suggesting that these two phases behave in a similar manner to that of the $\alpha + \delta$ pearlite phase. A change in slope has been observed to occur in other materials, and gives different values of the constants $A$ and $B$ in Equation 2, one set at low temperatures and another set at high temperatures [35]. This is generally taken to imply that different strengthening mechanisms are operative in these temperature ranges.

The interlamellar spacing/hardness relationships and the observation of the specimens deformed in tension give some confirmation of this hypothesis. At 293 K the hardness increased with decreasing interlamellar spacing, and metallographic observations showed the pearlite behaving essentially as a ductile–brittle composite with only limited deformation of the brittle $\delta$-phase possible before it cleaved and initiated final failure. Thus, at low temperatures the pearlite interfaces would appear to be strengthening the structure.

At higher temperatures, in the absence of interlamellar spacing/hardness data, some predictions about behaviour can be made by applying the Law of Mixtures in the form:

$$H_p = H_\alpha V_\alpha + H_\delta V_\delta \qquad (3)$$

where $H_p$, $H_\alpha$ and $H_\delta$ are the hardnesses of the pearlite, $\alpha$- and $\delta$-phases, respectively, and $V_\alpha$ and $V_\delta$ the volume fractions of these phases obtained from the phase diagram. Fig. 9b shows the calculated values, $H_p$, and the experimentally determined pearlite hardness, $H_{exp}$, plotted as a function of temperature. At temperatures below about 550 K $H_{exp}$ values are greater than $H_p$, while at higher temperatures the reverse is true. The experimental errors in measurement of the hardness of the pro-eutectoid $\alpha$- and $\delta$-phases make the experimental error in $H_p$ too large to say exactly how $H_p - H_{exp}$ varies with temperature up to 550 K, although it appears to be decreasing as the temperature increases. This trend implies that the strengthening effect of the pearlite interfaces is reduced at elevated temperatures. This would correspond to the gradient in the $H$ versus $\lambda^{-1/2}$ plot decreasing with temperature, a result which has been found for the NiAl–Cr fibrous eutectic [36]. Tensile testing at 658 K showed extensive deformation of the pearlite suggesting continuous deformation without a significant strengthening effect of the interfaces.

The fractography of the Cu–In alloy at room temperature is very similar to that reported previously for unidirectionally grown eutectics, for example, Al–$CuAl_2$ [37]. At 293 K the Cu–In alloy appears to behave in a manner analogous to a conventional fibre-reinforced material, with no plastic instability and the fracture surface perpendicular to the tensile axis. No change in slope of the stress–strain curve could be detected which would indicate a change from a primary modulus to a secondary modulus for a conventional fibre composite, but as the strain was measured from the cross-head movement any small deviations from linearity would be obscured by the machine compliance [38]. Failure is caused by the initial cracks in the brittle $\delta$-phase linking together by shear in the ductile $\alpha$-phase.

At 658 K both phases appear ductile and without the constraint of a reinforcing phase the stress–strain curve shows plastic instability with extensive necking leading to final shear failure. The exact nature of failure was not definitely established although from the presence and distribution of voids it is suspected that it takes place by the coalescence of voids formed at interphase boundaries.

## 5. Conclusions

(1) Significant hardness increases are achieved in unidirectionally heat-treated Cu–In eutectoids by the use of faster growth velocities which result in finer interlamellar spacing.

(2) The variation of hardness in the as-transformed eutectoid structures is best represented as being proportional $\lambda^{-1/2}$.

(3) The directionally transformed structure was cooled from the transformation temperature at rates in the range 0.047 to 18.6 K min$^{-1}$. These slow cooling rates could affect the strengthening mechanism by their influence on the extent of precipitation and/or coarsening in the supersaturated eutectoid phases.

(4) Anisotropy of hardness was found in the lamellar eutectoid structure, which is consistent with the anisotropy in properties found in lamellar

eutectics and indicative of useful unidirectional mechanical properties.

(5) Hot microhardness tests indicate different strengthening mechanisms above and below 550 K, probably related to the reduced strengthening effect of the pearlite interfaces at elevated temperatures.

(6) Tensile tests show that the room temperature deformation is limited by the ductile-brittle nature of the eutectoid composite but that at high temperatures the lamellar structure deforms as a continuum.

(7) The failure mechanism at room temperature is controlled by the linking-up of fractured $\delta$-lamellae, while at high temperatures a void coalescence mechanism is thought to be applicable.


## Acknowledgements

The authors are indebted to Professor R. W. K. Honeycombe for his continued interest and the provision of laboratory facilities. Sincere thanks are expressed to Professor G. A. Chadwick for his constant encouragement and helpful discussions and to the Science Research Council for their sponsorship. DVE wishes to thank the Royal Society for the Warren Research Fellowship.


## References


1. G. J. DAVIES, "Strengthening Methods in Crystals", edited by A. Kelly and R. B. Nicholson (Elsevier, London, 1971) p.485.
2. J. D. LIVINGSTON, *Composites* **4** (1973) 70.
3. G. J. DAVIES, "Practical Metallic Composites", (Institution of Metallurgists, London, 1974) p.D1.
4. M. J. SALKIND, F. D. LEMKEY and F. D. GEORGE, "Whisker Technology", edited by A. P. Levitt (Wiley, New York, 1967) p.343.
5. G. A. CHADWICK, *Acta Met.*, **24** (1976) 1137.
6. J. D. LIVINGSTON, *J. Mater. Sci.* **5** (1970) 951.
7. F. M. A. CARPAY, *Acta Met.* **18** (1970) 747.
8. D. CHEETHAM and N. RIDLEY, *Met. Trans.* **4** (1973) 2549.
9. B. G. MELLOR and G. A. CHADWICK, *Metal Sci.* **8** (1974) 65.
10. F. M. A. CARPAY, *Acta Met.* **20** (1972) 929.
11. D. CHEETHAM and N. RIDLEY, *J. Inst. Metals* **99** (1971) 371.
12. J. D. LIVINGSTON, *"In-Situ Composites"*, Vol. 1, (National Materials Advisory Board, Washington, 1973) p.87.
13. *Idem, Acta Met.* **23** (1975) 521.
14. G. F. BOLLING and R. H. RICHMAN, *Met. Trans.* **1** (1970) 2095.
15. G. A. CHADWICK and D. V. EDMONDS, symposium on Applications in Ferrous Metallurgy, Sheffield, 1971, published as Chemical Metallurgy of Iron and Steel, I.S.I. Special Report No. 146 (1973) p.264.
16. D. CHEETHAM and N. RIDLEY, *JISI* **211** (1973) 648.
17. B. G. MELLOR and D. V. EDMONDS, *Met. Trans.* **8A** (1977) 763.
18. *Idem, ibid* **8A** (1977) 773.
19. K. B. GOVE and J. A. CHARLES, *The Metallurgist* **6** (1973) 119.
20. G. A. CHADWICK, *"In-Situ* Composites", Vol. 2, (National Materials Advisory Board, Washington, 1976) p.474.
21. B. J. SHAW, *Acta Met.* **15** (1967) 1169.
22. I. G. DAVIES and A. HELLAWELL, *Phil. Mag.* **19** (1969) 1285.
23. H. E. CLINE and D. LEE, *Acta Met.* **18** (1970) 315.
24. E. R. THOMPSON, F. D. GEORGE and E. M. BREINAN, *"In-Situ* Composites", Vol. 2, (National Materials Advisory Board, Washington, 1973) p.71.
25. F. W. CROSSMAN, A. S. YUE and A. E. VIDOZ, *Trans. Met. Soc. AIME* **254** (1969) 397.
26. H. R. BERTORELLO and H. BILONI, *Met. Trans.* **3** (1972) 73.
27. M. GENSAMER, E. B. PEARSALL and G. V. SMITH, *Trans. ASM* **28** (1940) 380.
28. M. GENSAMER, E. B. PEARSALL, W. S. PELLINI and J. R. LOW, *ibid* **30** (1942) 983.
29. T. TAKAHASHI and M. NAGUMO, *Trans. Japan Inst. Metals* **11** (1970) 113.
30. S. JUSTI and R. H. BRAGG, *Met. Trans.* **6A** (1976) 1954.
31. H. BOHM, Z. Metallk. **50** (1959) 87.
32. *Idem, ibid* **52** (1961) 512.
33. D. J. H. CORDEROY and R. W. K. HONEYCOMBE, *J. Inst. Metals* **92** (1963) 65.
34. J. M. SHAPIRO and J. S. KIRKALDY, *Acta Met.* **16** (1968) 1239.
35. J. H. WESTBROOK, *Trans. ASM* **45** (1953) 221.
36. J. L. WALTER and H. E. CLINE, *Met. Trans.* **1** (1970) 1221.
37. B. CANTOR, G. J. MAY and G. A. CHADWICK, *J. Mater. Sci.* **8** (1973) 830.
38. A. R. T. DE SILVA, PhD Dissertation, University of Cambridge, 1969.


Received 11 May and accepted 25 July 1977.